

Martensitic transformation and microstructure of rapidly solidified $Ti_{50-x}Ni_{25}Cu_{25}Zr_x$ shape memory alloys

L. Litynska, Ph. Vermaut^{1,2}, J. Morgiel, J. Dutkiewicz, P. Ochin² and R. Portier^{1,2}

*Institute of Metallurgy and Materials Science of the Polish Academy of Sciences,
ul. Reymonta 25, 30-059 Krakow, Poland*

¹ *Laboratoire de Métallurgie Structurale, École Nationale Supérieure de Chimie de Paris,
11 rue Pierre et Marie Curie, 75231 Paris, France*

² *Centre d'Études de Chimie Métallurgique, UPR 2801 du CNRS, 15 rue G. Urbain,
94400 Vitry-sur-Seine, France*

Abstract. Addition of Zr up to 10 at% to $Ti_{50-x}Ni_{25}Cu_{25}Zr_x$ alloys has been used to elaborate melt spun ribbons. It has been found that low Zr content increase the glass forming ability of the alloy with a maximum at 2.5 % where the ribbon is almost fully amorphous. Above 2.5 at% a second crystalline phase occur which prevent martensitic transformation even in thermal treated samples. After crystallization, bimodal grain size distribution in low Zr content ribbons lead to a two-stage martensitic transformation. A decrease of the transformation temperature is observed with increasing Zr content. The increase of the martensitic transformation temperatures during aging is attributed to a plate-like precipitation.

1. INTRODUCTION

The transformation temperature of shape memory alloys is one of the most important parameters from the point of view of future applications. The alloying of NiTi with zirconium increases the transformation temperature range up to 300°C in alloys containing 20%Zr [1]. On the other hand it is reported that TiNiCu alloys show narrow transformation hysteresis [2]. Additionally, copper does not change significantly transformation temperature range [3]. Copper addition decreases also liquidus temperature of TiNi alloys and improves quality of melt spun ribbons causing partial amorphization of ribbons [4-8].

In the present paper the effect of zirconium on the amorphisation of $Ti_{50-x}Ni_{25}Cu_{25}Zr_x$ ribbons and the transformation temperature range in as cast, crystallized and annealed state are investigated.

2. EXPERIMENTAL

The ribbons were produced by a single-roller melt-spinning technique (planar flow). Melting and casting were performed under protective helium atmosphere. A copper wheel rotating with a linear speed of 19m/s was used for all castings with ejection pressure of 200 hPa. The melt spinning temperature varied from 1270 to 1310°C.

Heat treatments were carried out in a vacuum furnace ($p < 5 \cdot 10^{-6}$ torr). Characteristic temperatures of the martensitic transformation were determined by DSC measurements using a Mettler TA4000 calorimeter. Microstructure analysis was carried out by X-ray diffraction, TEM and optical microscopy. Etching for optical microscopy was made by exposure to a 10% H_2O_2 , 5% HF, 5% HCl, 80% H_2O solution. TEM investigations were made on a Topcon 002B high resolution electron microscope and a Philips CM20 equipped with Edax X-ray Energy Dispersion Spectrometry (EDS) attachment. Thin foils were prepared by twin jet electropolishing in a 6% perchloric acid in acetic acid solution at 14°C.

3. RESULTS AND DISCUSSION

The melt spun ribbons were 8-10mm wide and 30-50 μm thick. Those containing 0-2.5 at% Zr were ductile and with smooth surface while the ribbons containing 5 and 10 at% Zr were very brittle. The microstructure of the ribbons and their martensitic transformation characteristics were investigated in as

spun state and after the following thermal treatments: crystallization process at 450°C and annealing at 480°C.

3.1 As spun ribbons

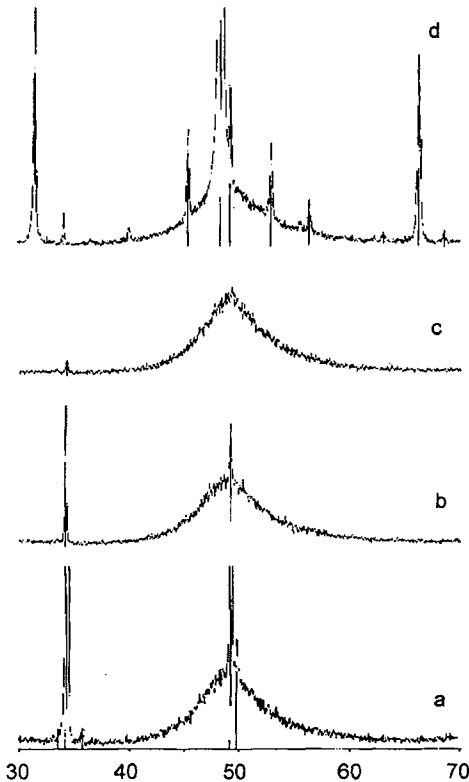


Figure 1 : The X - ray spectra from top side of the Ti50-xNi25Cu25Zrx ribbons a) $x=0$, b) $x=1$ c) $x=2.5$ d) $x=5$.

The X-ray diffraction showed presence of the amorphous phase in all as-spun ribbons. Its amount was higher on the top side than on the wheel side for all ribbons. Figure 1 shows that it also increases with the Zr content but only in the range $x = [0, 2.5 \text{ %}]$. For the higher Zr content the amount of the amorphous phase does not increase and a second phase forms as proved by peaks visible in Figure 1d.

In all ribbons and especially on the wheel side, reflections of B2 phase with preferred 100 orientation were observed. Only in ribbons containing 0 and 1%Zr additional weak martensite peaks are present.

Correlation between Zr content and amorphous phase amount was confirmed by optical microscopy of cross section as shown in Figure 2. The crystalline phase was present in the $x=[0-2.5\%Zr]$ ribbons as spherical patches mainly connected to the wheel side surface. However, in the ribbons with higher Zr content the crystalline phase was formed as a discontinuous thin layer on the wheel side. Etching of these ribbons resulted in reverse contrast (the crystalline phase is whiter while amorphous darker).



Figure 2 : Cross sectional optical micrograph of etched melt spun ribbons for the different compositions.

The DSC measurements of the as spun TiNiCuZr ribbons with different Zr additions are presented in Figure 3. All ribbons were first rapidly cooled to -150°C and then heated to 250°C at $10^{\circ}\text{C}/\text{min}$. The two thermal cycles heating and cooling were made for each sample but no differences between the first and second cycles were observed.

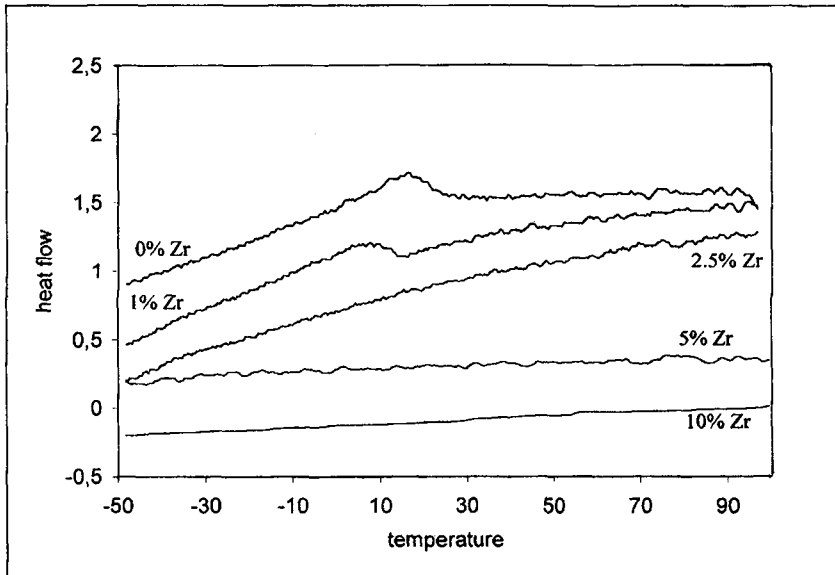


Figure.3: DSC cooling curves of NiTiCu and NiTiCuZr as spun ribbons.

The samples containing 0% and 1% of Zr showed weak one-stage transformation with a long tail on lower temperature side, while for 2.5% and higher Zr contents the heat flow was constant. The characteristic temperatures and latent heat of phase transitions measured from cooling and heating curves are presented in Table 1.

Table 1: Characteristic martensite temperatures in $^{\circ}\text{C}$ and transformation energy in J/g in as spun ribbons.

material	M_s	M_f	A_s	A_f	A_p	M_p	E
$x=0$	26	3	7	35	24	16	2
$X=1$	15	-	-	24	15	7	1.3

The above indicate that addition of Zr results in lowering of M_s temperature, what is in accordance with measurements published by Mulder [9] when Zr substitutes only Ti element in the ternary alloys

3.2 Crystallization

The in situ heating in DSC of the as spun ribbon from RT to 550°C at $20^{\circ}\text{C}/\text{min}$. are shown in Figure 4. The peak shapes for the low Zr content up to 2.5 % are well defined and the crystallization enthalpy per mass unit increases with the Zr content, which is consistent with the previous results. The broader peaks observed for the 5 and 10 % Zr may be attributed to the stresses caused by presence of the second phase. The plot of the crystallization temperature of melt spun ribbons versus Zr content show that they increase almost linearly with zirconium addition (Figure 5).

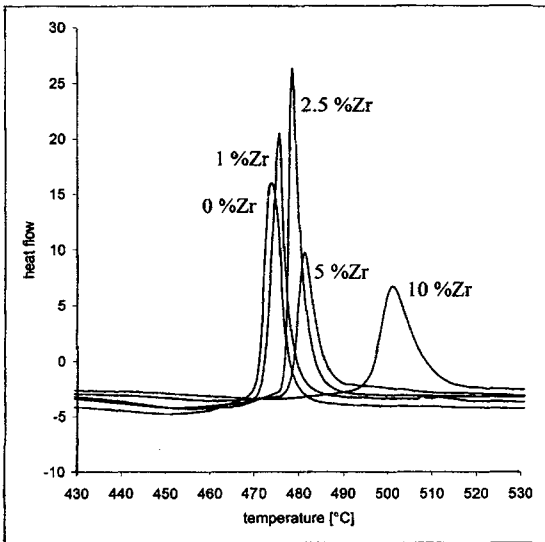


Figure 4 : DSC curves of the crystallization of the ribbons

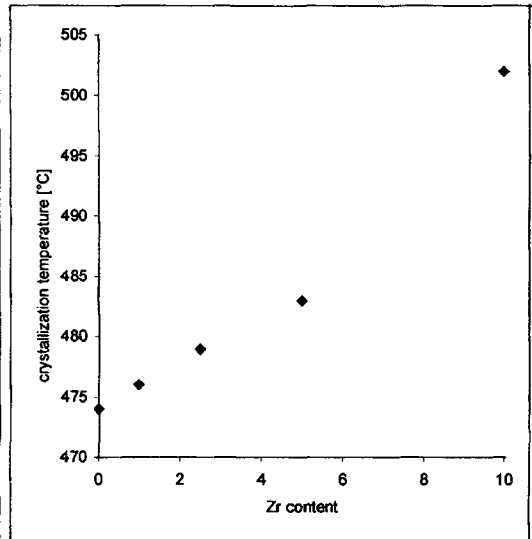


Figure 5 : The relationship of crystallization temperatures of melt spun ribbons vs Zr content [at%]

Two heating and cooling cycles between -100°C and 200°C were recorded at $10^{\circ}\text{C}/\text{min}$. after crystallization. The samples containing less than 2.5 % Zr show one or two transformation peaks. The transformation temperature shifts towards lower temperatures with increasing Zr content (Fig.6), but vanishes for ribbons containing 5 % or more addition of Zr.

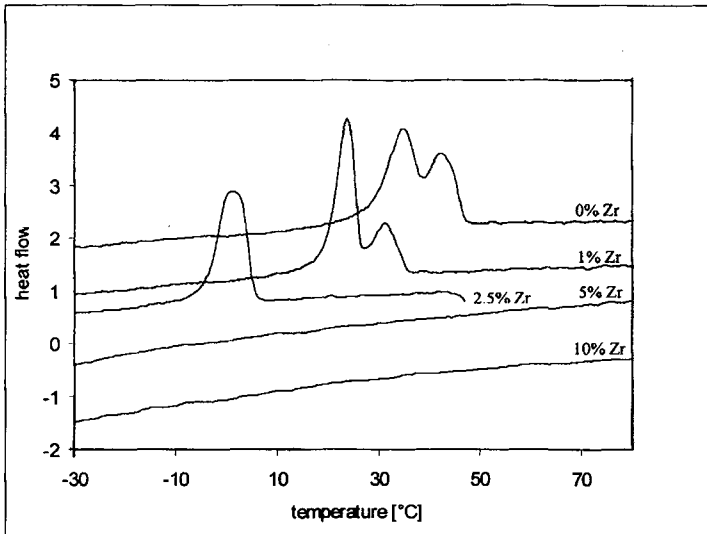


Figure.6 : DSC cooling curves - second cycle after crystallization.

The transformation temperatures and heat flow measured from the DSC curves are given in the Table 2. In correlation with the observation of the amount of amorphous phase, one can attribute the two stage martensitic transformation in alloys containing 0 and 1% Zr to the formation of fine grain β phase from the amorphous phase. Coarse grain and fine grains regions show different transformation temperature.

Table 2. Characteristic martensite temperatures in [°C] and transformation energy [J/g] in ribbons after crystallization in DSC.

material	Ms	Mf	As	Af	Ap	Mp	E
x = 0	47	27	40	55	49	35	11
x = 1	35	19	32	42	36	24	10
x = 2.5	6	-4	9	23	15	1	7

3.3 Annealing

The in-situ aging of the as-spun ribbons in the DSC apparatus was carried out at 450°C, i.e. just below the crystallization temperature. The cooling DSC curves for ribbons with 1 and 2.5% Zr content recorded after different annealing time are shown in Figure 7. For both compositions, annealing leads to a two-stage martensitic transformation. The heat flow of the higher temperature peak does not change significantly. The transformation temperature increases with the time of annealing as well as the heat flow. It seems that growth of the second (smaller) transformation peak is less pronounced.

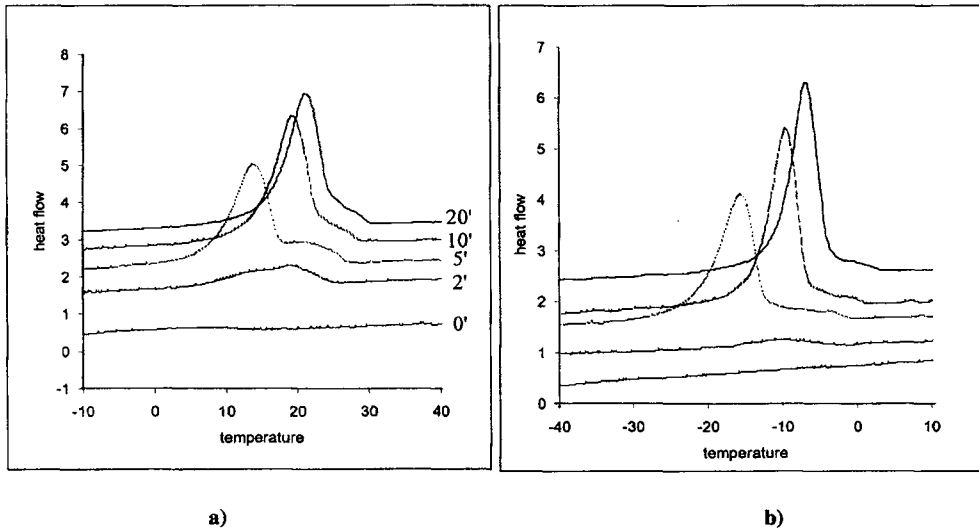


Figure 7: Cooling DSC curves after different time in situ annealing (0-20 min.) at 450°C a) 1%Zr b) 2.5%Zr

TEM investigations have been carried out in annealed ribbons. For all samples, a fine plate-like precipitation parallel to $\{001\}_{B2}$ planes is visible as shown in Figure 8. Selected area diffraction patterns are similar to those already reported by Rösner *et al.* [8]. In order to make the identification of these precipitates easier, long time of annealing, up to 100 hrs, have been carried out to make them grow. Line scan X-ray microanalysis across the precipitate plates (figure 9) allow to point out a Cu enrichment and Ni content decrease in these precipitates. Very small Ti content change was detected. As a consequence, the precipitation coarsening during annealing probably change the matrix composition and may influence the martensitic transformation temperature of the ribbons. Moreover, HREM investigations have pointed out strain field in the matrix around the plates which is a function of the size of the precipitates. Detailed results on this precipitation will be published in a forthcoming paper.



Figure 8 : HREM image along $[001]_{B2}$ of precipitation in a 10 hrs annealed 2.5% Zr content sample, with corresponding diffraction pattern

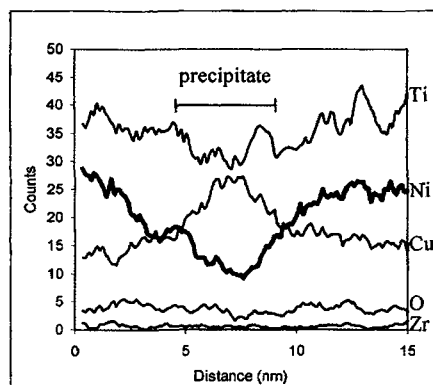


Figure 9 : X-ray microanalysis profile across a precipitate plate in a 100 hrs annealed sample.

4. CONCLUSIONS

1. The zirconium additions of up to 2.5 % into TiNiCu alloy result in nearly complete ribbon amorphization. Higher additions of 5 –10 % Zr cause formation of second crystalline phase in addition to B2.
2. The crystallization temperatures of the investigated alloys increase almost linearly with the zirconium content.
3. The as spun ribbons containing 0 – 1% Zr show weak martensitic transformation within temperature range 3 – 25°C. The heat of transformation increases after crystallization and the transformation appears in alloy containing 2.5% Zr. The martensitic transformation temperatures decrease with zirconium addition. The ribbons show two stage transformation what is due to presence of coarse crystallites formed during casting and fine formed during following crystallization of the amorphous phase.
4. The increase of the transformation temperatures observed after annealing is attributed to changes in matrix composition resulting from nucleation and coarsening of a plate-like precipitates, which contain more copper and less nickel than the matrix and follow $\langle 100 \rangle$ matrix directions.

Acknowledgement

The authors would like to thank A. Dezellus and Ph. Plaindoux for ribbons preparation. This work is supported by EEC INCO-Copernicus project IC15-CT96-0704.

References

1. J. H. Mulder, J. H. Mass, J. Beyer, Proc. ICOMAT 92, Monterey (1992) 869
2. T. H. Nam, T. Saburi, Y. Nakata, K. Shimizu, Mat. Trans. JIM, **31** (1990) 10504.
3. O. Mercier, K. N., Melton, Met. Trans., **10A** (1979) 387
4. M. N. Matveeva, V. A. Lobodjuk, V. I. Kolomycev, I. D. Lovcova, Metally (1991) 164
5. Y. Furuya, M. Matsumoto, T. Matsumoto, Proc. ICOMAT 92, Monterey (1992) 905
6. Z. L. Xie, J. van Humbeeck, Y. Liu, L. Delaey, Scripta Mat., **379** (1997) 363
7. J. Dutkiewicz, J. Morgiel, T. Czeppe, Proc. ICEM14, Mexico (1998) 29
8. H. Rösner, A. V. Shelyakov, A. M. Glezer, K. Feit, P. Schloßmacher, Mat. Sci. Eng., A **273-275** (1999) 733
9. J. H. Mulder, PhD Thesis, Twente University, Enschede (The Netherlands), (1995) 40